



## SIMULATION OF WAVE PROPAGATION ON THIN FILM

L. H. Wiryanto<sup>1</sup>, R. Widayawati<sup>2</sup>, R. Fauzi<sup>3</sup>, G. Putra<sup>3</sup> and E. Noviani<sup>4</sup>

<sup>1</sup>Department of Mathematics  
Institut Teknologi Bandung  
Indonesia  
e-mail: [leo@math.itb.ac.id](mailto:leo@math.itb.ac.id)

<sup>2</sup>Department of Civil Engineering  
University of Lampung  
Indonesia  
e-mail: [luh\\_ratnawidyawati@yahoo.co.id](mailto:luh_ratnawidyawati@yahoo.co.id)

<sup>3</sup>Department of Mathematics  
Institut Teknologi Sumatera  
Indonesia  
e-mail: [rifky.fauzi@ma.itera.ac.id](mailto:rifky.fauzi@ma.itera.ac.id); [gusrian.putra@ma.itera.ac.id](mailto:gusrian.putra@ma.itera.ac.id)

<sup>4</sup>Department of Mathematics  
University of Tanjungpura  
Indonesia  
e-mail: [evi\\_noviani@math.untan.ac.id](mailto:evi_noviani@math.untan.ac.id)

---

Received: June 14, 2022; Accepted: August 2, 2022

2020 Mathematics Subject Classification: 76A20, 76B15, 76D08.

Keywords and phrases: thin film, lubrication theory, forward time central space, stability condition.

---

How to cite this article: L. H. Wiryanto, R. Widayawati, R. Fauzi, G. Putra and E. Noviani, Simulation of wave propagation on thin film, *Advances and Applications in Fluid Mechanics* 29 (2022), 45-58. <http://dx.doi.org/10.17654/0973468622007>

This is an open access article under the CC BY license (<http://creativecommons.org/licenses/by/4.0/>).

Published Online: August 17, 2022

### Abstract

We are concerned with fluid having very small thickness flowing on an inclined bottom. The thickness of the fluid varies by changing time, so that it forms wave propagation, and we observe the wave profile. Since the fluid is thin, it can be modelled based on the theory of lubrication. We formulate the model into a single equation of the fluid thickness with the boundary conditions. The viscosity and the surface tension are two physical parameters considered in the wave evolution. The difficulty in solving the equation is strongly non-linearity of the model. Therefore, to deal with the non-linearity, we used a numerical approach, i.e., forward time central space (FTCS). The stability is analyzed before we apply it to the equation, so that we can simulate the wave. We obtain that the wave changes the form into almost shock.

### 1. Introduction

Surface wave is an interesting topic to be studied. Mathematical model has been derived by many researchers. KdV equation, Boussinesq equations or shallow water equations are typical models that can be found in literature. The governing equations are simplified into one of those models by special assumption. But for fluid with small thickness, much smaller than the wave length, the governing equations based on Navier-Stoke can be reduced into lubrication theory, see for example in Acheson [1].

Model of lubrication theory together with the boundaries is usually then formulated into a single equation, such as in King et al. [2] and Wiryanto and Febrianti [3]. In [2], the authors formulated the steady thin film into an integral equation involving a fast upward airflow. The interface pressure between both the fluids can be expressed in thin airfoil theory, such as in Van Dyke [4], so that the model becomes an integral equation.

Unsteady thin film on an inclined channel is studied by Wiryanto and Febrianti [3]. A partial differential equation of the fluid thickness is the model. When it is solved, the solution as surface wave propagating and changing the form could be observed. Decrease in the amplitude of the wave

occurred indicating that the front wave tends to shock. Wiryanto [5] and Wiryanto [6] then developed a finite difference method for that model to see the stability condition.

In this paper, we derive the model from the lubrication theory involving viscosity and surface tension. The model is then solved numerically, after analyzing the stability, so that we can simulate the wave deformation and propagation. The wave with almost jump can be obtained, similar to the simulation for shallow water model in Fauzi and Wiryanto [7] and Fauzi and Wiryanto [8], called to be the *roll wave*. This formation was also studied by Needham and Merkin [9], Merkin and Needham [10], and previously predicted by Dressler [11].

## 2. Wave Formulation

A thin fluid flowing down on an inclined channel is considered. The sketch of the flow is illustrated in Figure 1. The coordinates are chosen Cartesian with horizontal  $x$ -axis along the bottom of the channel and the vertical  $y$ -axis perpendicular to the other. Wave propagates on the surface expressed as the fluid thickness  $y = h(x, t)$  measured from the bottom. The flow in the thin fluid layer is taken to be governed by the lubrication equations, which are written as

$$\left. \begin{aligned} u_x + v_y &= 0 \\ -p_x + \mu u_{yy} + \rho g \sin \theta &= 0 \\ -p_y - \rho g \cos \theta &= 0 \end{aligned} \right\}. \quad (1)$$

All fluid quantities are written in the conventional notation. These equations are to be solved subject to the conditions

- (i)  $u = v = 0$  on  $y = 0$ ,
- (ii)  $u_y = 0$  on  $y = h(x, t)$ ,
- (iii)  $p = p_f$  on  $y = h(x, t)$ ,
- (iv)  $h_t + h_x u - v = 0$  on  $y = h(x, t)$ .

The fluid is non-slip at the bottom, expressed in condition (i), and the other three conditions are on the surface presenting no shear stress (ii). The pressure (iii) at the surface is presented by the atmospheric pressure, defined as the reference  $p_{atm} = 0$ , and the surface tension  $\gamma$  multiplied by the curvature approximated by the second derivative of the surface:

$$p = p_f \approx -\gamma \frac{\partial^2 h}{\partial x^2}.$$

Meanwhile, the kinematic condition is given in (iv).

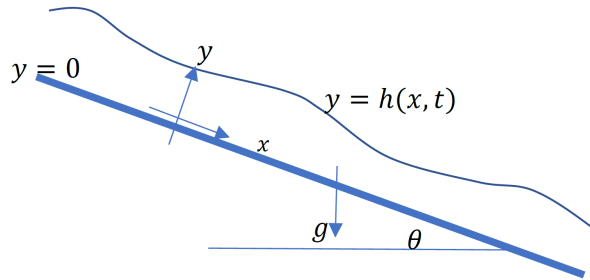


**Figure 1.** Sketch of the coordinates and the fluid flow.

Following Wiryanto and Febrianti [3], equations (1) and boundary conditions (i)-(iv) are readily integrated and it gives a single equation put in the form

$$h_t + \frac{\rho}{3\mu} \left[ h^3 \left( -h_x g \cos \theta + g \sin \theta + \frac{\gamma}{\rho g} h_{xxx} \right) \right]_x = 0. \quad (2)$$

The effect of the surface tension is presented in the last term, that was not involved in [3].

Equation (2) is a non-linear equation for the depth of the fluid layer measured from the inclined bottom of the channel. Therefore, the model can be used to observe the wave deformation and propagation, where the initial condition is required.

### 3. Stability Analysis

In solving (2), numerical approach is used as it is strongly non-linear. But we first analyze the stability. The constant solution is satisfied for any  $h = h_0$ . For small disturbance, we write the solution of the order  $\varepsilon$  in form of  $h(x, t) = h_0 + \varepsilon\eta(x, t)$ . When we substitute it into (2), the first order of  $\varepsilon$  is

$$\eta_t + (a\eta - b\eta_x + c\eta_{xxx})_x = 0, \quad (3)$$

where  $a = \rho g \sin \theta / \mu$ ,  $b = \rho g \cos \theta / 3\mu$ ,  $c = \gamma / 3\mu$ , they are all constants.

We first observe the solution in form of monochromatic wave

$$\eta(x, t) = Ae^{i(kx - \omega t)},$$

where  $k$  is the wave number, the frequency  $\omega$  is written in complex form  $\omega = \omega_r + i\omega_i$  for  $i = \sqrt{-1}$ , so that the wave can be expressed

$$\eta(x, t) = A_{mp}e^{i(kx - \omega_r t)}. \quad (4)$$

Here, the wave amplitude depends on time  $A_{mp} = Ae^{\omega_i t}$ . Now, we observe the characteristic of the wave by substituting (4) into (3), the real and imaginary parts are, respectively,

$$\omega_i + bk^2 + ck^4 = 0,$$

$$-\omega_r + ak = 0.$$

This gives  $\omega_i < 0$ , the wave decreases by increase in time.

A finite difference method is then applied to (3), by firstly integrating (3) at small interval  $[x_i, x_{i+1}]$ . The first term is approximated by

$$\int_{x_i}^{x_{i+1}} \eta_t dx \approx \eta_t \Big|_{x_{i+\frac{1}{2}}} \Delta x$$

and the other terms are approximated by centre space of the mid point  $x_{i+\frac{1}{2}}$ .

It is then shifted the index by writing  $k = i + \frac{1}{2}$ , similar method in Wiryanto and Febrianti [3], so that the finite difference equation is

$$\eta_k^{n+1} = \eta_k^n - \frac{\Delta t}{\Delta x} \left[ a \left\{ \frac{\eta_{k+1}^n + \eta_k^n}{2} - \frac{\eta_k^n + \eta_{k-1}^n}{2} \right\} - b \left\{ \frac{\eta_{k+1}^n - \eta_k^n}{\Delta x} - \frac{\eta_k^n - \eta_{k-1}^n}{\Delta x} \right\} \right] + \left[ \frac{\eta_{k+2}^n - 3\eta_{k+1}^n + 3\eta_k^n - \eta_{k-1}^n}{\Delta x^3} - \frac{\eta_{k+1}^n - 3\eta_k^n + 3\eta_{k-1}^n - \eta_{k-2}^n}{\Delta x^3} \right] \quad (5)$$

Note, we define  $\eta_k^n \approx \eta(x_k, t_n)$ , the value of  $\eta$  at discretization point  $(x_k, t_n)$ .

Stability condition can be analyzed by expressing

$$\eta_k^n = u^n e^{ik\varphi},$$

for any  $\varphi$ . This is then substituted into the finite difference equation above. The stability condition can be obtained when  $u$  satisfies  $|u| < 1$ . After some algebraic operations, we obtain the real and imaginary part of  $u$ , where  $u$  is written in complex form as  $u = u_r + iu_i$ . Each of the parts as follows:

$$u_r = 1 - \frac{\Delta t}{\Delta x^2} \left( 2b + \frac{4c}{\Delta x^2} \right) + \frac{\Delta t}{\Delta x} \left( \frac{2b}{\Delta x} + \frac{8c}{\Delta x^3} - \frac{4c}{\Delta x^3} \cos \varphi \right) \cos \varphi,$$

$$u_i = \frac{\Delta t}{\Delta x} a \sin \varphi.$$

To satisfy  $|u| < 1$ , the real and imaginary parts are written in ellipse

$$\left[ \frac{u_r - \left\{ 1 - \frac{\Delta t}{\Delta x^2} \left( 2b + \frac{4c}{\Delta x^2} \right) \right\}}{\frac{\Delta t}{\Delta x^2} \left( 2b + \frac{8c}{\Delta x^2} - \frac{4c}{\Delta x^2} \cos \varphi \right)} \right]^2 + \left[ \frac{u_i}{a \frac{\Delta t}{\Delta x}} \right]^2 = 1.$$

The centre of the ellipse is  $(A, 0)$ , where

$$A = 1 - \frac{\Delta t}{\Delta x^2} \left( 2b + \frac{4c}{\Delta x^2} \right).$$

The horizontal and vertical radii are

$$R_h = \frac{\Delta t}{\Delta x^2} \left( 2b + \frac{8c}{\Delta x^2} - \frac{4c}{\Delta x^2} \cos \varphi \right),$$

$$R_v = a \frac{\Delta t}{\Delta x}.$$

The ellipse has to be inside of the unit circle  $|u| < 1$ , i.e., if  $0 \leq A \leq 1$ ,  $R_h + A \leq 1$  for any  $\varphi$ , and  $R_v$  is not too large. Otherwise, some part of the ellipse is out of the unit circle. We illustrate that ellipse inside the unit circle in Figure 2. The ellipse with solid line indicates inside unit circle, with possible  $R_h + A \leq 1$ , and  $R_v$  not too large. But when  $R_v$  is larger, we obtain the ellipse with dash line. It is not expected.

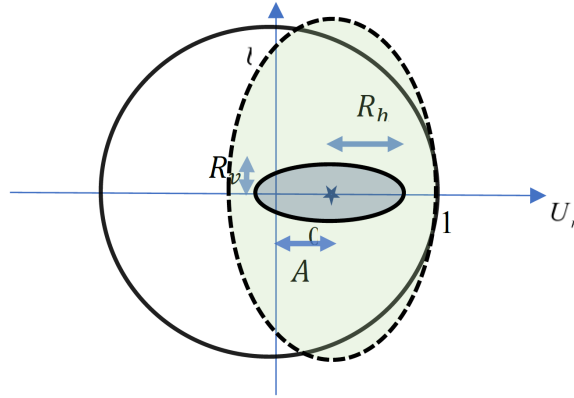


**Figure 2.** The stability area shown inside of the solid-line ellipse.

From  $0 \leq A \leq 1$ , we obtain

$$0 \leq \frac{\Delta t}{\Delta x^2} \left( 2b + \frac{4c}{\Delta x^2} \right) \leq 1. \quad (6)$$

Meanwhile  $R_h + A < 1$  gives

$$\frac{\Delta t}{\Delta x} \left( \frac{4b}{\Delta x} + \frac{8c}{\Delta x^3} \right) > 0.$$

This is then used in (6) to express the stability condition, written in form of

$$\Delta t \leq \frac{\Delta x^4}{4c + 2b\Delta x^2}. \quad (7)$$

We then simulate that analysis using  $g = 9.8$ ,  $\rho = 1$ ,  $\mu = 1$  and  $\gamma = 0.072$  for small angle  $\theta = 5$  degree. For  $dx = 0.1$ , the finite difference equation (5) would be stable when it is calculated using  $dt < 0.0006$ . In Figure 3, we show plot of our calculation using  $dt = 0.0001$  with initial value  $\eta_k^0 = \sin(2\pi x_k/50)$ .

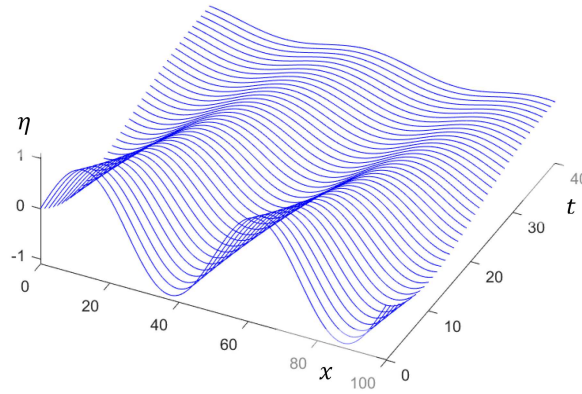


**Figure 3.** Plot of stable numerical calculation of  $\eta(x, t)$  using (5).

For some values of  $n$ , we plot  $\eta_k^n$  in 3D. Numerically, the curves change smoothly. The wave amplitude decreases by increasing the time. This agrees with our analysis described above.

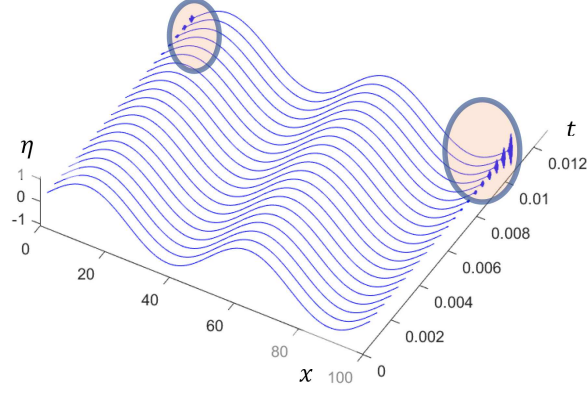


**Figure 4.** Plot of unstable numerical calculation of  $\eta(x, t)$  using (5).

Another plot of  $\eta_k^n$  is given in Figure 4, calculated using  $dt = 0.0005$ . We perform the unstable indication, shown inside of the circles, appearing wiggles. The numerical calculation is no longer run, as the wiggles increase rapidly.

#### 4. Numerical Solution

Based on the stability analysis, we develop the numerical procedure for (2) by integrating in a small interval  $[x_i, x_{i+1}]$ :

$$\int_{x_i}^{x_{i+1}} h_t dx + F \Big|_{x_i}^{x_{i+1}} = 0,$$

where  $F = \frac{\rho}{3\mu} h^3 \left( -h_x g \cos \theta + g \sin \theta + \frac{\gamma}{\rho g} h_{xxx} \right)$ . The first term is approximated by

$$\int_{x_i}^{x_{i+1}} h_t dx \sim h_t \Big|_{x_{i+\frac{1}{2}}} \Delta x \sim \frac{h_{i+\frac{1}{2}}^{n+1} - h_{i+\frac{1}{2}}^n}{\Delta t} \Delta x,$$

and the second term by

$$F \Big|_{x_i}^{x_{i+1}} = F \Big|_{x_{i+1}} - F \Big|_{x_i},$$

where

$$F|_{x_{i+1}} = \frac{\rho}{3\mu} \left( \frac{h^n_{i+\frac{3}{2}} + h^n_{i+\frac{1}{2}}}{2} \right)^3 \left[ -g \cos \theta \frac{h^n_{i+\frac{3}{2}} - h^n_{i+\frac{1}{2}}}{\Delta x} + g \sin \theta + \frac{\gamma}{\rho g} \frac{h^n_{i+\frac{5}{2}} - 3h^n_{i+\frac{3}{2}} + 3h^n_{i+\frac{1}{2}} - h^n_{i-\frac{1}{2}}}{\Delta x^3} \right]$$

and

$$F|_{x_i} = \frac{\rho}{3\mu} \left( \frac{h^n_{i+\frac{1}{2}} + h^n_{i-\frac{1}{2}}}{2} \right)^3 \left[ -g \cos \theta \frac{h^n_{i+\frac{1}{2}} - h^n_{i-\frac{1}{2}}}{\Delta x} + g \sin \theta + \frac{\gamma}{\rho g} \frac{h^n_{i+\frac{3}{2}} - 3h^n_{i+\frac{1}{2}} + 3h^n_{i-\frac{1}{2}} - h^n_{i-\frac{3}{2}}}{\Delta x^3} \right].$$

We then shift the index by writing  $k = i + \frac{1}{2}$ , so that we obtain the finite difference equation of (2), similar to (5) but involving non-linear terms.

Now, we present the numerical solution of the model (2). The physical quantities as used in the linear model in the previous section are used to calculate  $h_k^n$ . We show in Figure 5. The initial value is in sinusoidal form

$$h_k^0 = 0.2 + 0.05 \sin(2\pi x_k/50),$$

and we can see the evolution during the wave propagation. Here, we observe the wave propagation in the interval of two wavelengths. Therefore, the value at  $x = 0$  is repeated at  $x = 100$ . In Figure 6, we plot together between  $h_k^0$  and  $h_k^{5000}$  as indicated, to show the variation of the wave, the form and

the amplitude. The effect of non-linearity is performed. We can compare the plot in Figure 3.

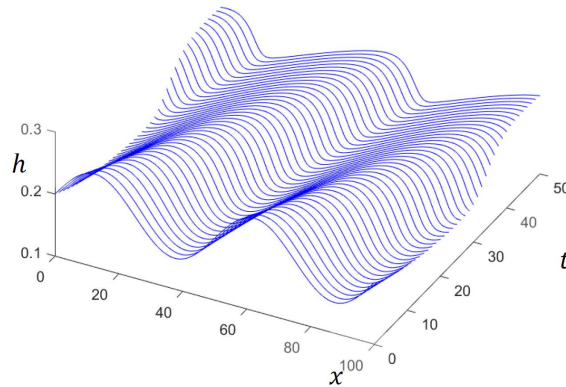


**Figure 5.** Plot of the numerical calculation of  $h(x, t)$ , as the solution of equation (2), using initial value  $h_k^0 = 0.2 + 0.05 \sin(2\pi x_k / 50)$ .

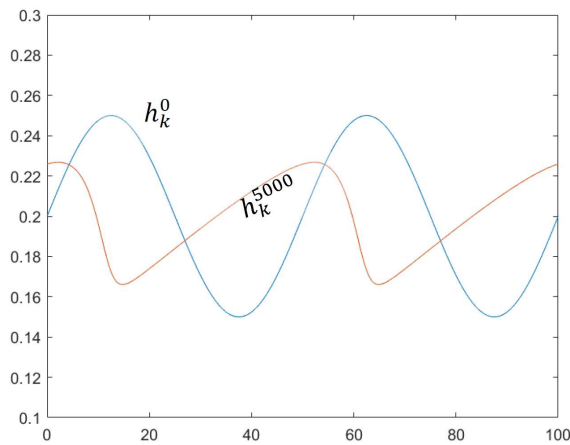


**Figure 6.** Plot of  $h_k^0$  and  $h_k^{5000}$  as indicated.

We then observe the effect of the inclination of the plane  $\theta$ . For longer  $\theta$ , we obtain that the wave reduces the amplitude faster, and the form tends to almost shock, i.e., sharp at the front wave. It indicates that the roll wave can be obtained in thin film flow, similar to such as in the references. We show in Figure 7 as the result of our calculation using  $\gamma = 0.1$  and  $\theta = 35^\circ$  (0.61 radian), with the same initial value as before. The shape of the wave

changes from sinusoidal into sharper at the front wave, compared to the previous calculation ( $\gamma = 0.072$  and  $\theta = 5^\circ$ ).

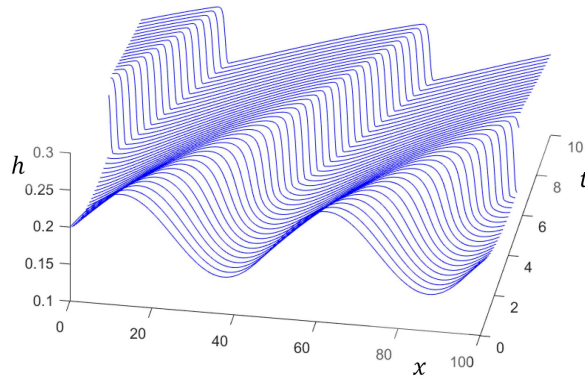


**Figure 7.** Plot of the numerical calculation of  $h(x, t)$ , as the solution of equation (2), using initial value  $h_k^0 = 0.2 + 0.05 \sin(2\pi x_k/50)$ ,  $\gamma = 0.1$  and  $\theta = 35^\circ$ .

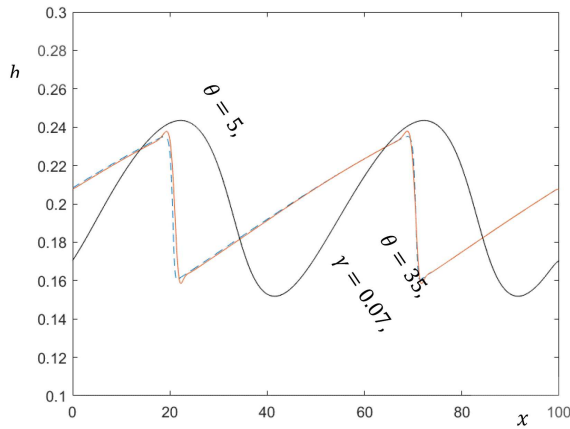


**Figure 8.** Plot of  $h_k^{1000}$  for  $\theta = 5^\circ$ ,  $\gamma = 0.07$  and  $\theta = 35^\circ$ ,  $\gamma = 0.07$  (dash line) almost the same for  $\theta = 35^\circ$ ,  $\gamma = 2.0$ .

For various values of surface tension  $\gamma$ , we obtain that for bigger  $\gamma$ , the numerical method gets difficult to calculate, it must be followed by using smaller step time  $\Delta t$ . However, this quantity slightly gives the same profile

for other values. We show this in Figure 8, plots of three  $h_k^{1000}$  from  $\theta = 5^\circ$ ,  $\gamma = 0.07$  and  $\theta = 35^\circ$ ,  $\gamma = 0.07$  (dash line) being almost the same as that from  $\theta = 35^\circ$ ,  $\gamma = 2.0$ . Therefore, the surface tension is less effective, and it can be neglected, so that the viscosity is the quantity that should be included in the model. Result for that model can be seen in references.

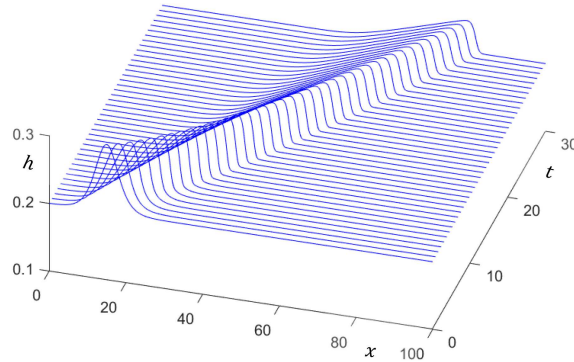


**Figure 9.** Plot of  $h(x, t)$ , as the solution of equation (2), using initial value  $h_k^0 = 0.2 + 0.1 \operatorname{sech}^2(0.25(x_k - 15))$ ;  $\mu = 3.0$  and  $\theta = 35^\circ$ .

For another initial wave, the numerical scheme is used to produce wave simulation as performed in Figure 9. The initial wave is solitary in form of

$$h_k^0 = 0.2 + 0.1 \operatorname{sech}^2(0.25(x_k - 15)).$$

This wave propagates on thin film of viscosity  $\mu = 3.0$  with bottom angle  $\theta = 35^\circ$ . We obtain that the amplitude decreases, followed by changing the form with the front wave becoming sharper.

## 5. Conclusion

A single equation model for surface wave on a thin fluid has been solved numerically. A finite difference method has been analyzed for stability condition, so that the method can be applied to solve the model, which can

simulate the wave propagation and the deformation. The physical quantities that play an important role are the inclination and viscosity, but surface tension is less effective in the model.

### References

- [1] D. J. Acheson, *Elementary Fluid Dynamics*, Oxford United Press, London, 1990, 245.
- [2] C. King, E. O. Tuck and J.-M. Vanden, Air-blown on thin viscous sheets, *Phys. Fluids A* 5 (1993), 973-978.
- [3] L. H. Wiryanto and W. Febrianti, Numerical solution of thin-film flowing down on an inclined channel, *Advances and Applications in Fluid Mechanics* 20(4) (2017), 595-604. doi: 10.17654/FM020040595.
- [4] M. Van Dyke, *Perturbation Methods in Fluid Mechanics*, Academic, New York, 1964.
- [5] L. H. Wiryanto, Stability analysis of thin film model, *IOP Conf Series: Journal of Physics: Conf. Series* 983 (2018), pp. 012072. doi: 10.1088/1742-6596/983/1/012072.
- [6] L. Wiryanto, A finite difference method for a thin film model, *Proc. Int. Conf. on Mechanical, Electrical and Medical Intelligent System (ICMEMIS)*, GS-02, 2017.
- [7] R. Fauzi and L. H. Wiryanto, On the staggered scheme for shallow water model down an inclined channel, *AIP Conf. Proc.* 1867 (2017), 020002-1-020002-8. doi: 10.1063/1.4994405.
- [8] R. Fauzi and L. H. Wiryanto, Predictor-corrector scheme for simulating wave propagation on shallow water region, *IOP Conf. Ser.: Earth Environ. Sci.* 162 (2018), pp. 012047.
- [9] D. J. Needham and J. H. Merkin, On roll waves down an open inclined channel, *Proc. R. Soc. Lond. A* 394 (1984), 259-278.
- [10] J. H. Merkin and D. J. Needham, An infinite periodic bifurcation arising in roll waves down an open inclined channel, *Proc. R. Soc. London Ser. A* 405 (1986), 103-116.
- [11] R. F. Dressler, Mathematical solution of problem of roll-waves in open inclined channels, *Commun. Pure Appl. Math.* 2 (1949), 149-194.